A Planar Catechin Analogue Having a More Negative Oxidation Potential than (+)-Catechin as an Electron Transfer Antioxidant against a Peroxyl Radical

Ikuo Nakanishi,[†,‡] Kei Ohkubo,[†] Kentaro Miyazaki,[§,∥] Wataru Hakamata,[§] Shiro Urano,[∥] Toshihiko Ozawa,[†] Haruhiro Okuda,[§] Shunichi Fukuzumi,*[,‡] Nobuo Ikota,*[,‡] and Kiyoshi Fukuhara*[,§]

Redox Regulation Research Group, Research Center for Radiation Safety, National Institute of Radiological Sciences, Inage-ku, Chiba 263-8555, Japan, Department of Material and Life Science, Graduate School of Engineering, Osaka University, CREST, Japan Science and Technology Agency, Suita, Osaka 565-0871, Japan, Division of Organic Chemistry, National Institute of Health Sciences, Setagaya-ku, Tokyo 158-8501, Japan, and Department of Applied Chemistry, Shibaura Institute of Technology, Minato-ku, Tokyo 108-8548, Japan

Received June 30, 2003

The hydrogen transfer reaction of antioxidative polyphenol with reactive oxygen species has proved to be the main mechanism for radical scavenging. The planar catechin (**P1H$_2$**), in which the catechol and chroman structure in (+)-catechin (**1H$_2$**) are constrained to be planar, undergoes efficient hydrogen atom transfer toward galvinoxyol radical, showing an enhanced protective effect against the oxidative DNA damage induced by the Fenton reaction. The present studies were undertaken to further characterize the radical scavenging ability of **P1H$_2$** in the reaction with cumylperoxyl radical, which is a model radical of lipid peroxyl radical for lipid peroxidation. The kinetics of hydrogen transfer from catechins to cumylperoxyl radical has been examined in propionitrile at low temperature with use of ESR, showing that the rate of hydrogen transfer from **P1H$_2$** is significantly faster than that from **1H$_2$**. The rate was also accelerated by the presence of Sc(OSO$_2$CF$_3$)$_3$. Such an acceleration effect of metal ion indicates that the hydrogen transfer reaction proceeds via metal ion-promoted electron transfer from **P1H$_2$** to oxyl radical followed by proton transfer rather than via a one-step hydrogen atom transfer. The electrochemical ease of **P1H$_2$** for the one electron oxidation investigated by second harmonic alternating current voltammetry strongly supports the two step mechanism for hydrogen transfer, resulting in the enhanced radical scavenging ability.

Introduction

Recently, much attention has been directed to the possibility of natural antioxidants, such as flavonoids, vitamin C, vitamin E, and β carotene, as chemopreventive agents against oxdative stress and associated diseases (*1*−*3*). The generation of free radicals, such as hydroxyl radical (•OH) and superoxide anion ($O_2^{\bullet-}$), in biological systems is regarded as an important event contributing to the oxidative stress phenomena and one associated with many diseases, e.g., inflammentation, heart disease, cancer, and Alzheimer's (*4*−*6*). Flavonoids are plant phenolic compounds, which are widely distributed in foods and beverages and are extensively studied for their antioxidative and cytoprotective properties in various biological models (*7*−*9*). The antioxidative effects of flavonoids are believed to come from their inhibition of free radical processes in cells at three different levels: an initiation, by scavenging of $O_2^{\bullet-}$ (*10*, *11*); lipid peroxidation, by reaction with peroxyl or lipid peroxyl radicals (*12*); and the formation of •OH, probably by chelating iron ions (*13*). Besides their beneficial effects, there is also considerable evidence that flavonoids themselves are mutagenic (*14*, *15*) or carcinogenic (*16*) and show DNA damaging activity (*17*, *18*). Quercetin is a typical flavonoid that has been investigated as a potential chemopreventive agent against certain carcinogens (*19*, *20*). The chemistry of quercetin is predictive of its free radical scavenging ability. However, in biological systems, it was clearly demonstrated that quercetin could behave as both antioxidant and prooxidant. That is, dietary administration of excess quercetin induced renal tubule adenomas and adenocarcinomas in male rats (*21*) and induced intestinal and bladder cancer in rats (*22*). As other polyphenolic compounds, flavonoids may not show the sufficient antioxidative effects into the cells because of their hydrophilic properties, which impede the cell membrane translocation step (*23*). Therefore, much consideration to the safety should be required, when a large quantity of flavonoid is used as medicine for cancer chemoprevention.

In addition to the studies of natural antioxidants used for cancer chemoprevention or nutrition supplements, development of novel antioxidants that show improved radical scavenging activities has attracted considerable interest to remove reactive oxygen species (ROS), such as $O_2^{\bullet-}$ and •OH (*24*). We have previously reported that a planar catechin derivative (**P1H$_2$**) (Figure 1), synthesized in the reaction of (+)-catechin (**1H$_2$**) with acetone

* To whom correspondence should be addressed. Tel: 81 3-3700 1141. Fax: 81-3 3707 6950. E-mail: fukuhara@nihs.go.jp.
† National Institute of Radiological Sciences.
‡ Osaka University, CREST, Japan Science and Technology Agency.
§ National Institute of Health Sciences.
∥ Shibaura Institute of Technology.

10.1021/tx034134c CCC: $27.50
Published on Web 12/03/2003

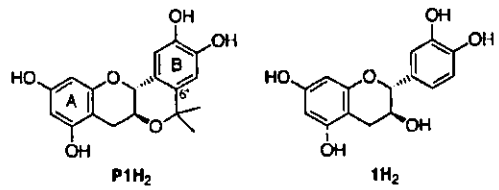

Figure 1. Chemical structures of planar catechin ($P1H_2$) and (+)-catechin ($1H_2$).

in the presence of $BF_3{\cdot}Et_2O$ (*25, 26*), shows an enhanced protective effect against the oxidative DNA damage induced by the Fenton reaction without the prooxidant effect, which is usually observed in the case of $1H_2$. The spectroscopic and kinetic studies have demonstrated that the rate of hydrogen transfer from $P1H_2$ to galvinoxyl radical (G$^{\bullet}$), a stable oxygen-centered radical, is about 5-fold faster than that of hydrogen transfer from the native $1H_2$ to G$^{\bullet}$ (*26*). We have also demonstrated that the $O_2^{\bullet-}$-generating ability of the dianion form of $P1H_2$ generated in the reaction of $P1H_2$ with 2 equiv of Bu_4NOMe in deaerated acetonitrile (MeCN) is much lower than that of $1H_2$, suggesting that $P1H_2$ may be a promising novel antioxidant with reduced prooxidant activity (*27*). In addition, as compared with the hydrophilic $1H_2$, the lipophilic property of $P1H_2$, which is very soluble in alcohol, ether, and tetrahydrofuran, seems to give rise to its antioxidative activity into cell membrane.

We report herein that $P1H_2$ can also scavenge cumylperoxyl radical ($PhCMe_2OO^{\bullet}$) more efficiently than $1H_2$. $PhCMe_2OO^{\bullet}$, while much less reactive than alkoxyl radicals, is known to follow the same pattern of relative reactivity with a variety of substrates (*28–30*). The effect of a metal ion on the rate of hydrogen transfer from $P1H_2$ to $PhCMe_2OO^{\bullet}$ was also examined in order to distinguish between the one-step hydrogen atom transfer and the electron transfer mechanisms in the radical scavenging reaction of $P1H_2$ (*31*). The one-electron oxidation potential (E_{ox}^0) of $1H_2$ as well as that of $P1H_2$ in MeCN was determined by the second-harmonic alternating current voltammetry (SHACV). The combination of kinetic and electrochemical results obtained in this study provides confirmative bases to develop novel antioxidants that show improved radical scavenging activities.

Materials and Methods

Materials. A planar catechin derivative ($P1H_2$) was synthesized according to the literature procedure (*26*). (+) Catechin ($1H_2$) was purchased from Sigma. Di-*tert*-butyl peroxide was obtained from Nacalai Tesque Co., Ltd., and purified by chromatography through alumina, which removes traces of the hydroperoxide. Cumene was purchased from Wako Pure Chemical Industries Ltd., Japan. Tetra-*n*-butylammonium perchlorate (TBAP) used as a supporting electrolyte was recrystallized from ethanol and dried under vacuum at 313 K. MeCN and propionitrile (EtCN) used as solvent were purified and dried by the standard procedure (*32*).

Spectral and Kinetic Measurements. Kinetic measurements for the hydrogen transfer reactions between catechins and cumylperoxyl radical were performed on a JEOL X-band spectrometer (JES-ME-LX) at 203 K. Typically, photoirradiation of an oxygen-saturated EtCN solution containing di-*tert*-butyl peroxide (1.0 M) and cumene (1.0 M) with a 1000 W high pressure Mercury lamp resulted in formation of cumylperoxyl radical ($PhCMe_2OO^{\bullet}$; g = 2.0156), which could be detected at low temperatures. The g values were calibrated by using an Mn^{2+} marker. Upon cutting off the light, the decay of the ESR intensity was recorded with time. The decay rate was accelerated by the presence of $P1H_2$ ($1.0 \cdot 10^{-4}$ M). Rates of hydrogen transfer from $P1H_2$ to $PhCMe_2OO^{\bullet}$ were monitored by measuring the decay of the ESR signal of $PhCMe_2OO^{\bullet}$ in the presence of various concentrations of $P1H_2$ in EtCN at 203 K. Pseudo first-order rate constants were determined by a least squares curve fit using an Apple Macintosh personal computer. The first order plots of $\ln(I - L)$ vs time (I and L are the ESR intensity at time t and the final intensity, respectively) were linear for three or more half lives with the correlation coefficient, $\rho > 0.99$. In each case, it was confirmed that the rate constants derived from at least five independent measurements agreed within an experimental error of ±5%.

Scheme 1

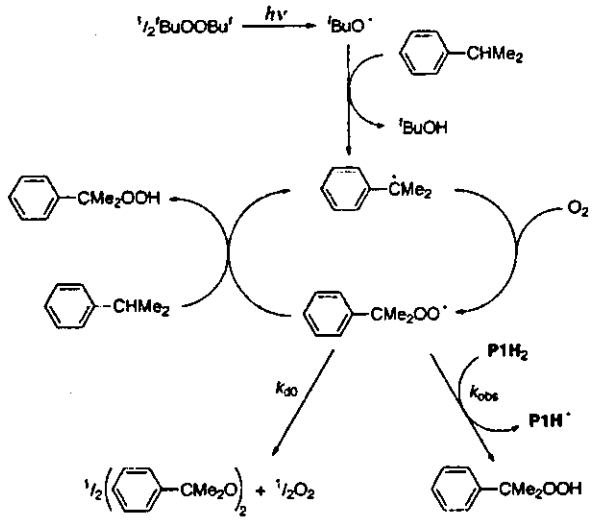

Electrochemical Measurements. The SHACV (*33–38*) measurements of $1H_2$ and $P1H_2$ were performed on an ALS 630A electrochemical analyzer in deaerated MeCN containing 0.10 M TBAP as a supporting electrolyte at 298 K. The platinum working electrode was polished with BAS polishing alumina suspension and rinsed with acetone before use. The counter electrode was platinum wire. The measured potentials were recorded with respect to an $Ag/AgNO_3$ (0.01 M) reference electrode. The one-electron oxidation potentials (E_{ox}^0) (vs $Ag/AgNO_3$) were converted into those vs SCE by addition of 0.29 V (*39*).

Results

Hydrogen Transfer from Catechins to Cumylperoxyl Radical. Direct measurements of the rates of hydrogen transfer from a planar catechin derivative ($P1H_2$) to cumylperoxyl radical were performed in EtCN at 203 K by means of ESR. The photoirradiation of an oxygen-saturated EtCN solution containing di-*tert*-butylperoxide (Bu^{t}OOBu^t) and cumene with a 1000 W high pressure mercury lamp results in formation of cumylperoxyl radical ($PhCMe_2OO^{\bullet}$), which was readily detected by ESR. The cumylperoxyl radical is formed via a radical chain process shown in Scheme 1 (*40–44*).

The photoirradiation of Bu^{t}OOBu^t results in the homolytic cleavage of the O–O bond to produce Bu^{t}O$^{\bullet}$ (*45–51*), which abstracts a hydrogen from cumene to give cumyl radical, followed by the facile addition of oxygen to cumyl radical. The cumylperoxyl radical can also abstract a hydrogen atom from cumene in the propagation step to yield cumene hydroperoxide, accompanied by regeneration of cumyl radical (Scheme 1) (*52, 53*). In the termination step, cumylperoxyl radicals decay by a bimolecular reaction to yield the corresponding peroxide

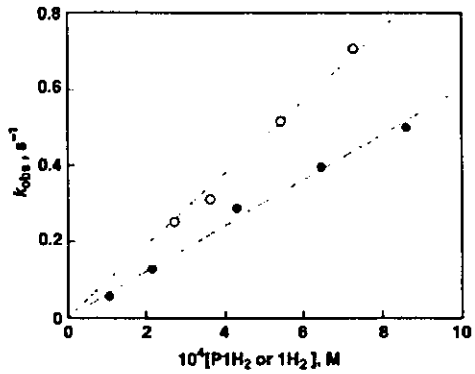

Figure 2. Plots of k_{obs} vs **P1H$_2$** (white circles) and vs **1H$_2$** (black circles) for the reactions of catechins (**P1H$_2$** and **1H$_2$**) with cumylperoxyl radical in EtCN at 203 K.

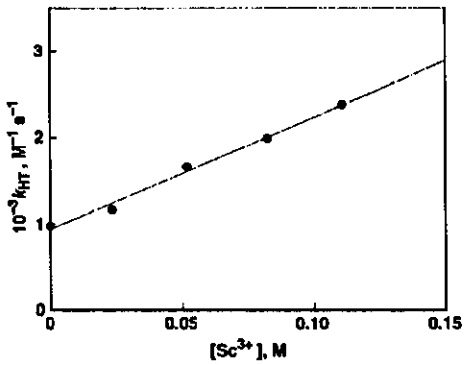

Figure 3. Plot of k_{HT} vs [Sc^{3+}] in the reaction of **P1H$_2$** to cumylperoxyl radical in the presence of $Sc(OSO_2CF_3)_3$ in EtCN at 203 K.

and oxygen (Scheme 1) (*41*, *42*). When the light is cut off, the ESR signal intensity decays obeying second-order kinetics due to the bimolecular reaction in Scheme 1.

In the presence of **P1H$_2$**, however, the decay rate of cumylperoxyl radical after cutting off the light becomes much faster than that in the absence of **P1H$_2$**. The decay rate in the presence of **P1H$_2$** (1.0×10^{-4} M) obeys pseudo first-order kinetics. This decay process is ascribed to hydrogen transfer from **P1H$_2$** to cumylperoxyl radical (Scheme 1). The pseudo-first-order rate constants increase with increasing **P1H$_2$** concentration ([**P1H$_2$**]) to exhibit first-order dependence on [**P1H$_2$**] as shown in Figure 2. From the slope of the linear plot of k_{obs} vs concentration of **P1H$_2$** is determined the second-order rate constant (k_{HT}) for the hydrogen transfer from **P1H$_2$** to cumylperoxyl radical as 9.7×10^2 M^{-1} s^{-1} in EtCN at 203 K.

Figure 2 also shows the linear plot of k_{obs} vs the concentration of (+)-catechin (**1H$_2$**) for the reaction of **1H$_2$** with cumylperoxyl radical in EtCN at 203 K. The k_{HT} value for **1H$_2$** was also determined in the same manner as 6.0×10^2 M^{-1} s^{-1} (*31*). Thus, as in the case of galvinoxyl radical (*26*), the hydrogen transfer rate from **P1H$_2$** to cumylperoxyl radical is significantly faster than that from **1H$_2$**.

We have recently reported that the hydrogen transfer from **1H$_2$** to galvinoxyl or cumylperoxyl radical proceeds via electron transfer from **1H$_2$** to galvinoxyl or cumylperoxyl radical, which is accelerated by the presence of metal ions, such as Mg^{2+} and Sc^{3+}, followed by proton transfer (*31*). In such a case, the coordination of the metal ion to the one-electron reduced species of galvinoxyl or cumylperoxyl radical may stabilize the product, resulting in acceleration of the electron transfer process. In this context, the effect of a metal ion on the k_{HT} value of **P1H$_2$** was examined. As in the case of **1H$_2$**, the hydrogen transfer from **P1H$_2$** to cumylperoxyl radical was significantly accelerated by the presence of $Sc(OSO_2CF_3)_3$ as shown in Figure 3. Thus, the hydrogen transfer from **P1H$_2$** to cumylperoxyl radical also proceeded via electron transfer from **P1H$_2$** to cumylperoxyl radical followed by proton transfer from **P1H$_2$**$^{\bullet+}$ to one-electron reduced species cumylperoxyl radical as shown in Scheme 2.

The larger k_{HT} value of **P1H$_2$** as compared to that of **1H$_2$** may be ascribed to the stability of the radical cation of **P1H$_2$** (**P1H$_2$**$^{\bullet+}$), which is produced in the electron transfer from **P1H$_2$** to cumylperoxyl radical. The electron donating *i*-propyl group at the B ring of **P1H$_2$** may

Scheme 2

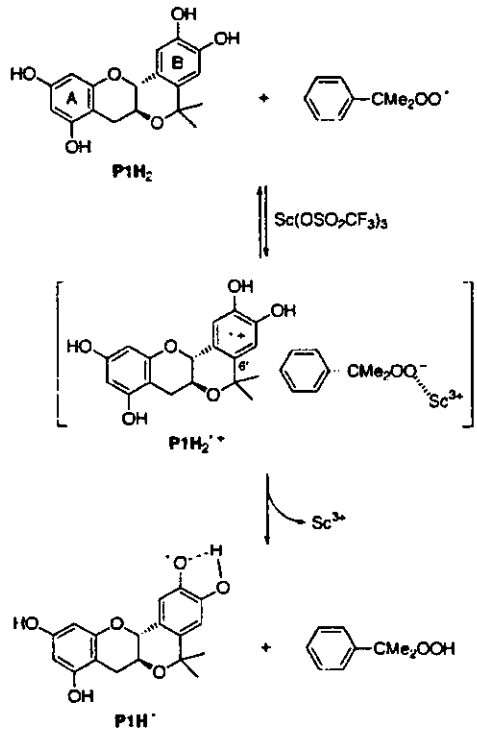

significantly stabilize **P1H$_2$**$^{\bullet+}$, resulting in the acceleration of the electron transfer step. In such a case, the one-electron oxidation potential of **P1H$_2$** is expected to be more negative than that of **1H$_2$**.

One-Electron Oxidation Potential of a Planar Catechin Analogue. To determine the one-electron oxidation potential of **P1H$_2$**, the cyclic voltammogram of **P1H$_2$** was recorded in MeCN containing 0.1 M TBAP as a supporting electrolyte at 298 K. Two irreversible oxidation (anodic) peaks were observed at 1.22 and 1.41 V vs SCE (data not shown). A similar cyclic voltammogram was obtained for **1H$_2$**, which exhibits irreversible oxidation peaks at 1.16 and 1.35 V vs SCE. This indicates that radical cations of **P1H$_2$** and **1H$_2$** are too unstable at the time scale of CV measurements. The SHACV method is known to provide a superior approach to directly evaluating one-electron redox potential in the presence of the follow-up chemical reaction relative to the better known dc and fundamental harmonic ac method (*34*). The

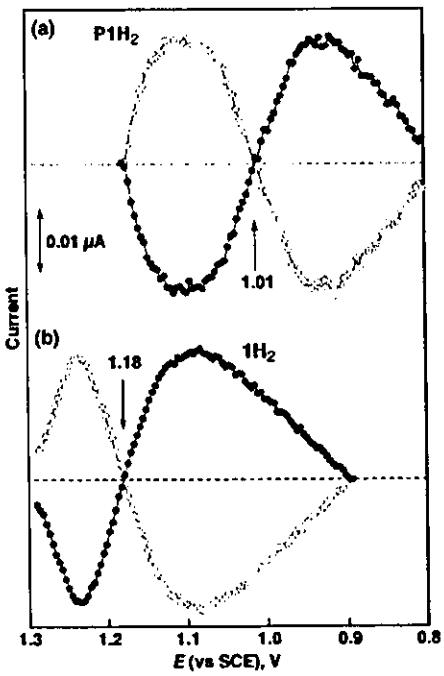

Figure 4. SHACVs of (a) $\mathbf{P1H_2}$ and (b) $\mathbf{1H_2}$ in deaerated MeCN containing 0.1 M TBAP at 298 K. Scan rate, 4 mV s^{-1}; working electrode, Pt.

SHACV method was applied to determine the one-electron oxidation potentials (E_{ox}^0) of $\mathbf{P1H_2}$ and $\mathbf{1H_2}$ in deaerated MeCN containing 0.1 M TBAP at 298 K. Figure 4 shows the SHACV of $\mathbf{P1H_2}$ and $\mathbf{1H_2}$. The E_{ox}^0 value of $\mathbf{P1H_2}$ thus determined (1.01 V vs SCE) is significantly more negative than that of $\mathbf{1H_2}$ (1.18 V vs SCE) as expected above. Thus, $\mathbf{P1H_2}$ may undergo one-electron oxidation by cumylperoxyl radical more easily than $\mathbf{1H_2}$, showing excellent radical scavenging abilities.

Discussion

The primary goal of this project is to develop a novel antioxidant, which can be positively utilized for clinical treatment and/or chemoprevention of diseases associated with ROS. There are two kinds of strategy in considering the development of synthetic antioxidants: one is a design of a new type of antioxidant, the structure of which is different from the natural antioxidant, and the other is a modification of natural antioxidants to improve its antioxidative capacities. A recent topic on the synthetic antioxidants is a development and clinical application of edaravone (3 methyl-1-phenyl-2 pyrazolin 5-one, MCI-186). Edaravone has been reported to show potent free radical scavenging actions toward ROS, such as $O_2^{\bullet-}$, H_2O_2, and HClO, which may be involved in the tissue destructive effects of reperfusion after ischemia (*54*−*56*). As a neuroprotective agent, edaravone has been clinically prescribed in Japan since 2001 to treat patients with cerebral ischemia. Regarding flavonoids, there are many reports for the synthetic derivatives to exert prominent chemopreventive effects toward oxidative stress-derived injury. However, only a few studies on the synthetic flavonoids, which were aimed at the improved radical scavenging ability, have been reported. Flavopiridol is a chlorinated derivative of flavone, which is currently in clinical development for the treatment of advanced cancer, including ovarian cancer (*57*, *58*). Flavopiridol is an inhibitor of cycline-dependent kinases to modulate cell cycle (*59*), and radical scavenging mechanism is not involved in the expression of anticancer effects of this compound.

The planar catechin ($\mathbf{P1H_2}$), which has been detected in mere trace amounts in nature (*60*), is easily synthesized by the reaction of $\mathbf{1H_2}$ and acetone (*26*). The ability of $\mathbf{P1H_2}$ to scavenge oxygen-centered radical, such as galvinoxyl radical, is excellent as compared to that of (+)-catechin and its complete inhibition of oxidative DNA damage induced by metal-catalyzed generation of hydroxyl radical (*26*), as well. Therefore, $\mathbf{P1H_2}$ may exert its antioxidative capacities by scavenging reactive oxygen radicals in many types of biologically generating systems. The present study was focused on the reaction of $\mathbf{P1H_2}$ to cumylperoxyl radical, a model radical of lipid peroxyl radical formed in a radical chain reaction of lipid peroxidation. The processes of lipid peroxidation concomitant with the formation of lipid peroxyl radicals are detrimental to the viability of the cell. The biophysical consequences of peroxidation on membrane phospholipids can be both extensive and highly destructive, provoking diseased states such as atherosclerosis, heart attacks, cancer, ischaemia/repulsion injury, and even the aging process as a whole (*61*). The ability of antioxidant to scavenge peroxyl radicals and block lipid peroxidation raises the possibility that it may protect against the many types of free radical associated diseases. As compared with $\mathbf{1H_2}$, $\mathbf{P1H_2}$ showed strong radical scavenging ability toward cumylperoxyl radical formed via a radical chain process, as well as the predominant radical scavenging reaction of $\mathbf{P1H_2}$ to galvinoxyl radical. Lipid peroxyl radical formed by the reaction between a lipid radical and a molecular oxygen is essential for autoxidation of lipid. The peroxyl radical abstracts an allylic hydrogen atom from an adjacent polyunsaturated fatty acid, resulting in a lipid hydroperoxide and a second lipid radical. Therefore, $\mathbf{P1H_2}$ may act as an effective terminator by means of scavenging free radicals in autoxidation of lipids.

Considering the antioxidative mechanism to scavenge peroxyl radical, there are two possibilities in the mechanism of hydrogen transfer reactions, i.e., a one step hydrogen atom transfer or electron transfer followed by proton transfer. The hydrogen transfer reaction from $\mathbf{P1H_2}$ to cumylperoxyl radical accelerated in the presence of the metal ion, indicating that the hydrogen transfer reaction proceeded by the two-step reaction, that is, electron transfer from $\mathbf{P1H_2}$ to cumylperoxyl radical followed by proton transfer from $\mathbf{P1H_2}^{\bullet+}$. Vitamin E is a typical antioxidant to terminate lipid peroxidation, and the hydrogen transfer reaction proceeds via a one-step hydrogen atom transfer process, which is due to no effect of metal ion on the hydrogen transfer rate from vitamin E analogue to galvinoxyl radical (*62*). On the other hand, in the case of $\mathbf{1H_2}$, the hydrogen transfer reaction proceeds via electron transfer from $\mathbf{1H_2}$ to oxyl radical followed by proton transfer rather than via a one step hydrogen atom transfer (*31*), as the case of present results of the $\mathbf{P1H_2}$. The one-electron oxidation potential investigated by the SHACV indicated that the electrochemical oxidation of $\mathbf{P1H_2}$ was easier to progress in comparison with $\mathbf{1H_2}$. The electron transfer mechanism for the radical scavenging reaction of $\mathbf{P1H_2}$ is probably a consequence of its electrochemical ease for one-electron oxidation. Judging from the one-electron oxidation po

tential of $\mathbf{P1H_2}$ that is higher than the one-electron reduction potential of cumylperoxyl radical ($E_{red}^0 = 0.65$ V vs SCE) (*63*), the free energy changes of electron transfer from $\mathbf{P1H_2}$ to cumylperoxyl radical are positive [ΔG_{et}^0 (in eV) $= e(E_{ox}^0 - E_{red}^0) > 0$, where e is elementary charge]; thereby, the electron transfer step is endergonic. In such a case, the initial electron transfer rate (k_{et}) may be the rate determining step in the overall rate of hydrogen transfer, which consists of electron and proton transfer steps. The maximum k_{et} value is evaluated from the ΔG_{et}^0 value by eq 1, where it is assumed that the activation free energy ($\Delta G_{et}^{\ddagger}$) is equal to ΔG_{et}^0 (no additional barrier is involved). Z is the frequency factor taken as 1×10^{11} M^{-1} s^{-1}, and k_B is the Boltzmann constant (*64, 65*).

$$k_{et} = Z \exp(-\Delta G_{et}^0 / k_B T) \qquad (1)$$

The maximum k_{et} value is calculated as 1.2×10^2 M^{-1} s^{-1}, which is the same order of magnitude as the observed k_{HT} value (9.0×10^2 M^{-1} s^{-1}). The larger k_{HT} value than the k_{et} value indicates that the hydrogen transfer from $\mathbf{P1H_2}$ to cumylperoxyl radical proceeds via a rate determining electron transfer with an interaction between $\mathbf{P1H_2}$ and cumylperoxyl radical. The formation of charge transfer complexes between cumylperoxyl radical and a variety of electron acceptors has been well documented in the literature (*66, 67*). Thus, the hydrogen transfer may proceed via an inner-sphere electron transfer in the charge transfer complex formed between $\mathbf{P1H_2}$ and cumylperoxyl radical. The acceleration of the hydrogen transfer rate in the presence of Sc^{3+} (Figure 3) is ascribed to the promoting effect of Sc^{3+} on the electron transfer step due to the strong binding of Sc^{3+} with cumylperoxyl anion produced in the electron transfer.

In conclusion, the hydrogen transfer from $\mathbf{P1H_2}$ to cumylperoxyl radical generated in radical chain reactions proceeds via an electron transfer reaction and the rate of hydrogen transfer from $\mathbf{P1H_2}$ to cumylperoxyl radical is faster than that from $\mathbf{1H_2}$. The predominance of $\mathbf{P1H_2}$ in the hydrogen transfer reaction is consistent with the electrochemical ease for its one electron oxidation potential. Since $\mathbf{P1H_2}$ is very lipophilic as compared to (+)-catechin itself, it is proposed that $\mathbf{P1H_2}$ interacts and penetarates the lipid bilayer giving rise to its maximized antioxidant capacity. Therefore, we believe that $\mathbf{P1H_2}$ may be significantly more effective not only for protecting tissue from the onslaught of the radical species governing peroxidation but also for terminating the autoxidation, which plays in provoking diseased states. Studies are underway to investigate basic biochemical properties of $\mathbf{P1H_2}$ in vivo, as well as to investigate its ability to serve as an antioxidant for the treatment of diseases associated with oxidative stress.

Acknowledgment. This work was partially supported by a Grant-in-Aid for Scientific Research Priority Area (No. 11228205) and a Grant-in-Aid for Young Scientist (B) (No. 15790032) from the Ministry of Education, Culture, Sports, Science and Technology, Japan, partly by a Grant (MF 16) from the Organization for Pharmaceutical Safety and Research, and by a Grant in-Aid for the Scientific Research (No. 14141201) from the Ministry of Health Labor and Welfare.

References

(1) Marchioli, R. (1999) Antioxidant vitamins and prevention of cardinovascular disease: laboratory, epidemiological and clinical trial data. *Pharmacol. Res. 40*, 227−238.

(2) Colic, M., and Pavelic, K. (2000) Molecular mechanisms of anticancer activity of natural dietetic products. *J. Mol. Med. 78*, 333−336.

(3) Willis, M. S., and Wians, F. H. (2003) The role of nutrition in preventing prostate cancer: a review of the proposed mechanism of action of various dietary substances. *Clin. Chim. Acta 330*, 57−83.

(4) Jadhav, S. J., Nimbalkar, S. S., Kulkarni, A. D., and Madhavi, D. L. (1996) Lipid oxidation in biological and food systems. In *Food Antioxidants* (Madhavi, D. L., Deshpande, S. S., and Salunkhe, D. K., Eds.) pp 5−63. Deller, New York.

(5) Sies, H. (1987) *Oxidative Stress*, Academic Press, London.

(6) Katzman, R., and Kawas, C. (1994) The epidemiology of dementia and Alzheimer's disease. In *Alzheimer Disease* (Terry, R. D., Katzman, R., and Bick, K. L., Eds.) pp 103−119. Raven Press, New York.

(7) Cody, V., Middleton, E., and Harborne, J. B. (1986) *Plant Flavonoids in Biology and Medicine: Biochemical Pharmacological and Structure−Activity Relationships*, Alan R. Liss, New York.

(8) Middleton, E., Jr., and Kandaswami, C. (1993) The impact of plant flavonoids on mammalian biology: implications for immunity, inflammation and cancer. In *The Flavonoids: Advances in Research Since 1986* (Harborne, J. H., Ed.) pp 619−652, Chapman and Hall, New York.

(9) Rice-Evance, C. A., Miller, N. J., and Paganga, G. (1996) Structure antioxidant activity relationships of flavonoids and phenolic acids. *Free Radical Biol. Med. 20*, 933−956.

(10) Jovanovic, S. V., Steenken, S., Tosic, M., Marjanovic, B., and Simic, M. G. (1994) Flavonoids as antioxidants. *J. Am. Chem. Soc. 116*, 4846−4851.

(11) Hu, J. P., Calomme, M., Lasure, A., De Bruyne, T., Pieters, L., Vlietinck, A., and Vanden Berghe, D. A. (1995) Structure−activity relationships of flavonoids with superoxide scavenging ability. *Biol. Trace Elem. Res. 47*, 327−331.

(12) Terao, J., Piskula, M., and Yao, Q. (1994) Protective effect of epicatechin, epicatechin gallate and quercetin on lipid peroxidation in phospholipids bilayers. *Arch. Biochem. Biophys. 308*, 278−284.

(13) Morel, J., Lescoat, G., Cogrel, P., Sergent, O., Pasdeloup, N., Brissot, P., Cillard, P., and Cillard, J. (1993) Antioxidant and iron-chelating activities of the flavonoids catechin, quercetin and diosmetin on iron-loads rat hepatocyte cultures. *Biochem. Pharmacol. 45*, 13−19.

(14) Sugimura, T., Nagao, M., Matsushima, T., Yahagi, T., Seino, Y., Shirai, A., Sawamura, M., Natori, S., Yoshihira, K., Fukuoka, M., and Kuroyanagi, M. (1977) Mutagenicity of flavone derivatives. *Proc. Jpn. Acad. B 53*, 194−197.

(15) Ochiai, M., Nagao, M., Wakabayashi, K., and Sugimura, T. (1984) Superoxide dismutase acts an enhancing factor for quercetin mutagenesis in rat liver cytosol by preventing its decomposition. *Mutat. Res. 129*, 19−24.

(16) Das, A., Wang, J. H., and Lien, E. J. (1994) Carcinogenicity, mutagenicity and cancer preventing activities of flavonoids: a structure system activity relationship (SSAR) analysis. *Prog. Drug Res. 42*, 133−166.

(17) Sahu, S. C., and Washington, M. C. (1991) Effects of antioxidants on quercetin-induced nuclear DNA damage and lipid peroxidation. *Cancer Lett. 60*, 259−264.

(18) Duthie, S. J., Johnson, W., and Dobson, V. L. (1997) The effect of dietary flavonoids on DNA damage (strand breaks and oxidized pyrimidines) and growth in human cells. *Mutat. Res. 390*, 141−151.

(19) Verma, A. K., Johnson, J. A., Gould, M. N., and Tanner, M. A. (1988) Inhibition of 7,12-dimethylbenz[*a*]anthracene and *N*-nitrosomethylurea induced rat mammary cancer by dietary flavonol quercetin. *Cancer Res. 48*, 5754−5758.

(20) Deschner, E. E., Ruperto, J., Wong, G., and Newmark, H. L. (1991) Quercetin and rutin as inhibitors of azoxymethanol induced colonic neoplasia. *Carcinogenesis 12*, 1193−1196.

(21) *Toxicology and Carcinogenesis Studies of Quercetin in F344 Rats* (1992) National Toxicology Program (NTP) Technical Report, NTP TR 409, NIH Publication No. 93-147478, National Institutes of Health, Bethesda, MD.

(22) Pamukcu, A. M., Yalciner, S., Hatcher, J. F., and Bryan, G. T. (1980) Quercetin, a rat intestinal and bladder carcinogen present in bracken fern (*Pteridium aquilinum*). *Cancer Res. 40*, 3468−3472.

(23) Kandaswami, C., Perkins, E., Soloniuk, D. S., Drzewiecki, G., and Middleton, E., Jr. (1991) Antiproliferative effects of citrus flavonoids on a human squamous cell carcinoma in vitro. *Cancer Lett. 56*, 147−152.

(24) Yoshikawa, T., Toyokuni, S., Yamamoto, Y., and Naito, Y. (2000) *Free Radical in Chemistry, Biology and Medicine*, OICA International (U.K.) Ltd., London.
(25) Guiso, M., Marra, C., and Cavarischia, C. (2001) Isochromans from 2-(3′,4′-dihydroxylphenylethanol. *Tetrahedron Lett. 42*, 6531–6534.
(26) Fukuhara, K., Nakanshi, I., Kansui, H., Sugiyama, E., Kimura, M., Shimada, T., Urano, S., Yamaguchi, K., and Miyta, N. (2002) Enhanced radical-scavenging activity of a planar catechin analogue. *J. Am. Chem. Soc. 124*, 5952–5953.
(27) Fukuhara, K., Nakanishi, I., Shimada, T., Ohkubo, K., Miyazaki, K., Hakamata, W., Urano, S., Ozawa, T., Okuda, H., Miyata, N., Ikota, N., and Fukuzumi, S. (2003) A planar catechin analogue as a promising antioxidant with reduced prooxidant activity. *Chem. Res. Toxicol. 16*, 81–86.
(28) Russel, G. A. (1973) Reactivity, selectivity, and polar effects in hydrogen atom transfer reactions. In *Free Radicals* (Kochi, J. K., Ed.) pp 275–331, John Wiley & Sons, New York.
(29) Russel, G. A. (1956) The rates of oxidation of aralkyl hydrocarbons. Polar effects in free radical reactions. *J. Am. Chem. Soc. 78*, 1047–1054.
(30) Howard, J. A., Ingold, U. K., and Symonds, M. (1968) Absolute rate constants for hydrocarbon oxidation VIII. Reactions of cumylperoxyl radicals. *Can. J. Chem. 46*, 1017–1022.
(31) Nakanishi, I., Miyazaki, K., Shimada, T., Ohkubo, K., Urano, S., Ikota, N., Ozawa, T., Fukuzumi, S., and Fukuhara, K. (2002) Effects of metal ions distinguishing between one step hydrogen and electron-transfer mechanisms for the radical-scavenging reaction of (+) catechin. *J. Phys. Chem. A 106*, 11123–11126.
(32) Perrin, D. D., Armarego, W. L. F., and Perrin, D. R. (1988) *Purification of Laboratory Chemicals*, Pergamon Press, Elmsford, New York.
(33) McCord, T. G., and Smith, D. E. (1969) Second harmonic a.c. polarography. Theoretical predictions for systems with first-order chemical reactions following the charge transfer step. *Anal. Chem. 41*, 1423–1441.
(34) Bond, A. M., and Smith, D. E. (1974) Direct measurement of $E_{T/2}$ with reversible EC electrode processes by second harmonic alternating current polarography and voltammetry. *Anal. Chem. 46*, 1946–1951.
(35) Wasielewski, M. R., and Breslow, R. (1976) Thermodynamic measurements on unsubstituted cyclopropenyl radical and anion, and derivatives by second harmonic alternating current voltammetry of cyclopropenyl cations. *J. Am. Chem. Soc. 98*, 4222–4229.
(36) Arnett, E. M., Amarnath, K., Harvey, N. G., and Cheng, J.-P. (1990) Determination and interrelation of bond heterolysis and homolysis energies in solution. *J. Am. Chem. Soc. 112*, 344–355.
(37) Patz, M., Mayr, H., Maruta, J., and Fukuzum, S. (1995) Reactions of carbocations with π nucleophiles: polar mechanism and no outer sphere electron-transfer processes. *Angew. Chem., Int. Ed. Engl. 34*, 1225–1227.
(38) Fukuzumi, S., Satoh, N., Okamoto, T., Yasui, K., Suenobu, T., Seko Y., Fujitsuka, M., and Ito, O. (2001) Change in spin state and enhancement of redox reactivity of photoexcited states of aromatic carbonyl compounds by complexation with metal ion salts acting as Lewis acids. Lewis acid catalyzed photoaddition of benzyltrimethylsilane and tetramethyltin via photoinduced electron transfer. *J. Am. Chem. Soc. 123*, 7756–7766.
(39) Mann, C. K., and Barnes, K. K. (1970) *Electrochemical Reactions in Non Aqueous Systems*, Mercel Dekker, New York.
(40) Sheldon, R. A. (1993) In *The Activation of Dioxygen and Homogeneous Catalytic Oxidation* (Barton, D. H. R., Martell, A. E., and Sawyer, D. T., Eds.) pp 9–30, Plenum Press, New York and London.
(41) Parshall, G. W., and Ittel, S. D. (1992) *Homogeneous Catalysis*, 2nd ed., Chapter 10, Wiley, New York.
(42) Sheldon, R., and Kochi, J. K. (1976) Metal catalyzed oxidations of organic compounds in the liquid phase: a mechanistic approach. *Adv. Catal. 25*, 272–413.
(43) Shilov, A. E. (1984) *Activation of Saturated Hydrocarbons by Transition Metal Complexes*, Chapter 4, D. Reidel Publishing Co., Dordrecht, The Netherlands.
(44) Böttcher, A., Birnbaum, E. R., Day, M. W., Gray, H. B., Grinstaff, M. W., and Labinger, J. A. (1997) How do electronegative substituents make metal complexes better catalysts for the oxidation of hydrocarbons by dioxygen? *J. Mol. Catal. A 117*, 229–242.
(45) Kochi, J. K. (1957) *Free Radicals in Solution*, John Wiley & Sons, New York.
(46) Kochi, J. K., Krusic, P. J., and Eaton, D. R. (1969) Homoallylic rearrangement and electron spin resonance of cyclopropylcarbinyl radicals. *J. Am. Chem. Soc. 91*, 1877–1879.
(47) Kochi, J. K., and Krusic, P. J. (1968) Electron spin resonance of aliphatic hydrocarbon radicals in solution. *J. Am. Chem. Soc. 90*, 7155–7157.
(48) Kochi, J. K., and Krusic, P. J. (1969) Electron spin resonance of organosilyl radicals in solution. *J. Am. Chem. Soc. 91*, 3938–3940.
(49) Kochi, J. K., and Krusic, P. J. (1969) Electron spin resonance studies of hemolytic substitution reactions. Oraganoboron, aluminum, and gallium compounds. *J. Am. Chem. Soc. 91*, 3942–3944.
(50) Kochi, J. K., and Krusic, P. J. (1969) Displacement of alkyl groups from organophosphorus compounds studied by electron spin resonance. *J. Am. Chem. Soc. 91*, 3944–3946.
(51) Howard, J. A., and Furimsky, E. (1974) Electron spin resonance study on the *tert*-butylsulfinyl radical. *Can. J. Chem. 52*, 555–556.
(52) Fukuzumi, S., and Ono, Y. (1977) Decay kinetics of cumylperoxyl radical produced by the decomposition of cumene hydroperoxide. *J. Chem. Soc., Perkin Trans. 2*, 622–625.
(53) Fukuzumi, S., and Ono, Y. (1977) Electron spin resonance and kinetic studies on the liquid-phase autoxidation of cumene with lead dioxide. *J. Chem. Soc., Perkin Trans. 2*, 784–788.
(54) Watanabe, T., Yuki, S., Egawa, M., and Nishi, H. (1994) Protective effects of MCI-186 on cerebral ischemia: possible involvement of free radical scavenging and antioxidant actions. *J. Pharmacol. Exp. Ther. 268*, 1597–1604.
(55) Yamamoto, T., Yuki, S., Watanabe, T., Mitsuya, M., and Saito, K. (1997) Delayed neuron death prevented by inhibition of increased hydroxyl radical formation in a transient cerebral ischemia. *Brain Res. 762*, 240–242.
(56) Okatani, Y., Wakatsuki, A., Enzan, H., and Miyahara, Y. (2003) Edaravone protects against ischemia/reperfusion-induced oxidative damage to mitochondria in rat liver. *Eur. J. Pharmacol. 465*, 163–170.
(57) Thomas, J. P., Tutsch, K. D., Cleary, J. F., Bailey, H. H., Arzoomanian, R., Alberti, D., Simon, K., Feierabend, C., Binger, K., Marnocha, R., Dresen, A., and Wilding, G. (2002) Phase I clinical and pharmacokinetic trial of the cyclin-dependent kinase inhibitor flavopiridol. *Cancer Chemother. Pharmacol. 50*, 465–472.
(58) Kouriukis, C. T., Belch, A., Crump, M., Eisenhauer, E., Gascoyne, R. D., Meyer, R., Lohmann, R., Lopez, P., Powers, J., Turner, R., and Connors, J. M. (2003) Flavopiridol in untreated of relapsed mantle-cell lymphoma: results of a phase II study of the National Cancer Institute of Canada Clinical Trials Group. *J. Clin. Oncol. 21*, 1740–1745.
(59) Senderowicz, A. M. (2002) Cyclin-dependent kinases as new targets for the prevention and treatment of cancer. *Hematol. Oncol. Clin. North Am. 16*, 1229–1253.
(60) Ngnokam, D., Massiot, G., Nuzillard, J. M., and Tsamo, E. (1994) (+)-7′,7′-Dimethyl 5-hydroxy 2R,3S trans-pubeschin from *Entandrophragma cylindricum*. *Phytochemistry 37*, 529–531.
(61) Davis, K. J. A. (1996) Oxidative stress: The paradox of aerobic life. *Biochem. Soc. Symp. 61*, 1–31.
(62) Nakanishi, I., Fukuhara, K., Shimada, T., Ohkubo, K., Iizuka, Y., Inami, K., Mochizuki, M., Urano, S., Itoh, S., Miyata, N., and Fukuzumi, S. (2002) Effects of magnesium ion on kinetic stability and spin distribution of phenoxyl radical derived from a vitamin E analogues: mechanistic insight into antioxidative hydrogen transfer reaction of vitamin E. *J. Chem. Soc., Perkin Trans. 2*, 1520–1524.
(63) Fukuzumi, S., Shimoosako, K., Suenobu, T., and Watanabe, Y. (2003) Mechanism of hydrogen-, oxygen-, and electron-transfer reactions of cumylperoxyl radical. *J. Am. Chem. Soc. 125*, 9074–9082.
(64) Itoh, S., Kumei, H., Nagatomo, S., Kitagawa, T., and Fukuzumi, S. (2001) Effects of metal ions on physicochemical properties and redox reactivity of phenolates and phenoxyl radicals: mechanistic insight into hydrogen atom abstraction by phenoxyl radical metal complexes. *J. Am. Chem. Soc. 123*, 2165–2175.
(65) Itoh, S., Maruta, J., and Fukuzumi, S. (1996) Addition-cyclization reaction of nitroalkane anions with *o*-quinone derivatives via electron transfer in the charge-transfer complexes. *J. Chem. Soc., Perkin Trans. 2*, 1429–1433.
(66) Boozer, C. E., and Hammond, G. S. (1954) Molecular complex formation in free radical reactions. *J. Am. Chem. Soc. 76*, 3861–3862.
(67) Boozer, C. E., Hammond, G. S., Hamilton, C. E., and Sen, J. N. (1955) Air oxidation of hydrocarbons. II. The stoichiometry and fate of inhibitors in benzene and chlorobenzene. *J. Am. Chem. Soc. 77*, 3233–3237.

TX034134C

Available online at www.sciencedirect.com
SCIENCE DIRECT
Mutation Research 559 (2004) 83–95
Genetic Toxicology and Environmental Mutagenesis
www.elsevier.com/locate/gentox
Community address: www.elsevier.com/locate/mutres

In vivo mutagenicity of benzo[*f*]quinoline, benzo[*h*]quinoline, and 1,7-phenanthroline using the *lacZ* transgenic mice

Katsuya Yamada[a], Takayoshi Suzuki[b], Arihiro Kohara[a,b], Makoto Hayashi[b], Takaharu Mizutani[a], Ken-Ichi Saeki[a,*]

[a] *Graduate School of Pharmaceutical Sciences, Nagoya City University, Tanabedori, Mizuho-ku, Nagoya 467-8603, Japan*
[b] *Division of Genetics and Mutagenesis, National Institute of Health Sciences, 1-18-1 Kamiyoga, Setagaya-ku, Tokyo 158-8501, Japan*

Received 25 September 2003; received in revised form 26 December 2003; accepted 26 December 2003

Abstract

Phenanthrene, a simplest angular polycyclic aromatic hydrocarbon with a bay-region in its molecule, is reported to be non-mutagenic, although most angular (non-linear) polycyclic aromatic hydrocarbons, such as benzo[*a*]pyrene and chrysene, are known to show genotoxicity after metabolic transformation into a bay-region diol epoxide. On the other hand, benzo[*f*]quinoline (BfQ), benzo[*h*]quinoline (BhQ), and 1,7-phenanthroline (1,7-Phe), which are all aza-analogs of phenanthrene, are mutagenic in the Ames test using *Salmonella typhimurium* TA100 in the presence of a rat liver S9 fraction. In this report, we undertook to investigate the in vivo mutagenicity of BfQ, BhQ and 1,7-Phe by an in vivo mutation assay system using the *lacZ* transgenic mouse (Muta™Mouse). BfQ and BhQ only slightly induced mutation in the liver and lung, respectively. BfQ- and BhQ-induced *cII* mutant spectra showed no characteristics compared with that of the control. These results suggest that the in vivo mutagenicities of BfQ and BhQ were equivocal. On the other hand, 1,7-Phe induced a potent mutation in the liver and a weak mutation in the lung. Furthermore 1,7-Phe depressed the G:C to A:T transition and increased the G:C to C:G transversion in the liver like quinoline, a hepatomutagen possessing the partial structure of 1,7-Phe, compared with the spontaneous mutation spectrum. These results suggest that the in vivo mutagenicity of 1,7-Phe might be caused by the same mechanism as that of quinoline, which induced the same mutational spectrum change (G:C to C:G transversion).

Keywords: Tricyclic aza-arene; In vivo mutagenesis assay; Mutation spectrum

1. Introduction

Carcinogenic aza-arenes are widely distributed in the environmental pollutants such as cigarette smoke [1] and urban air [2–4]. Although numerous studies about the in vitro mutagenicity of aza-arenes have been reported, the metabolic activation mechanism of aza-arenes has not yet been elucidated, except for that of heterocyclic amines. Furthermore, there are only a few reports about the in vivo mutagenicity of aza-arenes. We have investigated the in vitro and in vivo mutagenicity of aza-arenes with special attention to their metabolic activation mechanisms. 10-Azabenzo[*a*]pyrene, a carcinogenic aza-analog [5] of benzo[*a*]pyrene, was reported to be as mutagenic as benzo[*a*]pyrene in the Ames test using *Salmonella typhimurium* TA100 in the presence of a rat liver S9 fraction [6–8]. In our previous study,

* Corresponding author. Tel.: +81-52-836-3485; fax: +81-52-834-9309.
E-mail address: saeki@phar.nagoya-cu.ac.jp (K.-I. Saeki).

1383-5718/$ – see front matter
doi:10.1016/j.mrgentox.2003.12.012

Fig. 1. Structures of BfQ, BhQ and 1,7-Phe.

10-azabenzo[*a*]pyrene showed signi. cant mutagenicity only in the liver and colon in an in vivo mutation assay system using the *lacZ* transgenic mouse (Muta^{TM}Mouse) [9]. We have also reported that the total dose of 200 mg/kg (50 mg/kg per day × 4 days) of quinoline, a hepatocarcinogenic [10,11] aza-analog of naphthalene, showed a potent mutagenicity and induced primarily G:C to C:G transversions in the liver of Muta^{TM}Mouse [12–14].

Phenanthrene, a simplest angular polycyclic aromatic hydrocarbon with a bay-region in its molecule, has been reported to be non-mutagenic [15], although most angular (non-linear) polycyclic aromatic hydrocarbons, such as benzo[*a*]pyrene and chrysene, are known to show genotoxicity after metabolic transformation into a bay-region diol epoxide. On the other hand, it was reported that benzo[*f*]quinoline (BfQ) and 1,7-phenanthroline (1,7-Phe) (Fig. 1), which are environmental contaminants and aza-analogs of phenanthrene, were mutagenic in the Ames test using *S. typhimurium* TA100 in the presence of a rat liver S9 fraction [16–18]. Furthermore, benzo[*h*]quinoline (BhQ) (Fig. 1), a positional isomer of BfQ, was reported to be weakly or equivocally mutagenic in *S. typhimurium* TA100 with a rat liver S9 fraction [19,20]. In our previous report, it was suggested that metabolic activation of these tricyclic aza-arenes might take place in the pyridine moiety, like quinoline, to form the ultimate genotoxic form, an enamine epoxide (*N*,d-hydrated a,b-epoxide) (Fig. 2) [18].

In the present study, we undertook to investigate the in vivo mutagenicity of BfQ, BhQ and 1,7-Phe by the in vivo mutation assay system using the *lacZ* transgenic mouse (Muta^{TM}Mouse).

2. Materials and methods

2.1. Materials

BfQ (CAS Registry No. 85-02-9) and BhQ (CAS Registry No. 230-27-3) were purchased from Tokyo Kasei Kogyo Co. Ltd. (Tokyo), 1,7-Phe (CAS Registry No. 230-46-6) from Aldrich, phenyl-β-D-galactoside (P-gal) from Sigma Chemical Co. (St. Louis, MO, USA), proteinase K and olive oil from Wako Pure Chemicals (Osaka), and RNase from Boeringer Mannheim.

2.2. In vivo mutagenesis assay using Muta^{TM}Mouse

2.2.1. Animals and treatments

Seven-week-old male Muta^{TM}Mice, supplied by COVANCE Research Products (PA, USA), were acclimatized for 1 week before use and divided into seven groups of four mice each. BfQ, BhQ, and 1,7-Phe dissolved in olive oil (10 ml/kg body weight) were injected intraperitoneally into two, one, and two groups, respectively, at single doses of 100, 100, and 50 mg/kg, respectively, for four consecutive days. The remaining two groups were given olive oil as the control.

2.2.2. Tissues and DNA isolation

All mice were killed by cervical dislocation 14 days (BfQ-, BhQ-, 1,7-Phe- and olive oil-treated groups) or 56 days (BfQ-, 1,7-Phe- and olive oil-treated groups) after the last injection of a test chemical. The liver, spleen, lung, kidney, and bone marrow were immedi-

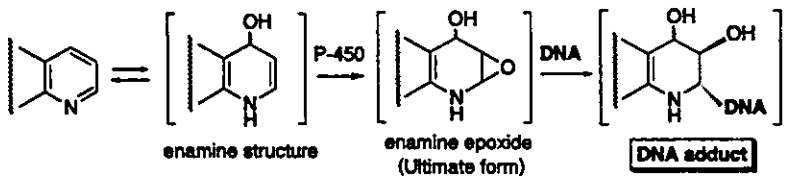

Fig. 2. Proposed metabolic activation pathway for the pyridine moiety (enamine epoxide theory).

ately extirpated, frozen in liquid nitrogen, and stored at −80 °C until DNA extraction. The genomic DNA was extracted from each tissue by the phenol/chloroform method as previously reported [12]. The isolated DNA was precipitated with ethanol, air-dried, and dissolved in an appropriate volume (20–200 μl) of TE-4 buffer (10 mM Tris–HCl at pH 8.0 containing 4 mM EDTA) at room temperature overnight. The DNA solution thus prepared was stored at 4 °C.

2.2.3. In vitro packaging

The lambda gt10/*lacZ* vector was ef. ciently recovered by the in vitro packaging reactions [21]. Our home-made (HM) packaging extract consisting of a sonic extract (SE) of *Escherichia coli* NM759 and a freeze–thaw lysate (FTL) of *E. coli* BHB2688 was prepared according to the methods of Gunther et al. [22]. As the general procedure for handling the HM extract, approximately 5 μg DNA was mixed with 15 μl of FTL and 30 μl of SE and incubated at 37 °C for 90 min. Then the SE and FTL were combined again and the mixture was incubated for another 90 min. The reaction was terminated by the addition of an appropriate volume of SM buffer (50 mM Tris–HCl at pH 7.5, 10 mM $MgSO_4$, 100 mM NaCl, 0.01% gelatin) and stored at 4 °C. By this procedure, the λgt10 vector was ef. ciently rescued from genomic DNA to form an infectious phage.

2.2.4. Mutation assays

2.2.4.1. lacZ mutant frequency determination. The positive selection for *lacZ* mutants was performed as previously reported [12,23]. Brie. y, the phage solution was absorbed to *E. coli* C (*lac*$^-$ *galE*$^-$) at room temperature for 20–30 min. For titration, an aliquot of the phage-*E. coli* solution was mixed with LB top agar (containing 10 mM $MgSO_4$) and plated onto dishes containing bottom agar. The remaining phage-*E. coli* solution was mixed with LB top agar containing phenyl-β-D-galactoside (P-gal) (3 mg/ml) and plated as described above. The mutant frequency (MF) was calculated by the following formula:

$$\text{mutant frequency} = \left(\frac{\text{total number of plaques on selection plates}}{\text{total number of plaques on titer plates}}\right) \times \text{dilution factor.}$$

The signi. cance of differences in the mutant frequency between the treated and control groups was analyzed by using Student's *t*-test.

2.2.4.2. cII mutant frequency determination. We also examined the mutagenicity in the lambda *cII* gene integrated as a lambda vector gene, which serves as another selective marker as reported previously in the *lacI* transgenic BigBlue mouse [24]. The positive

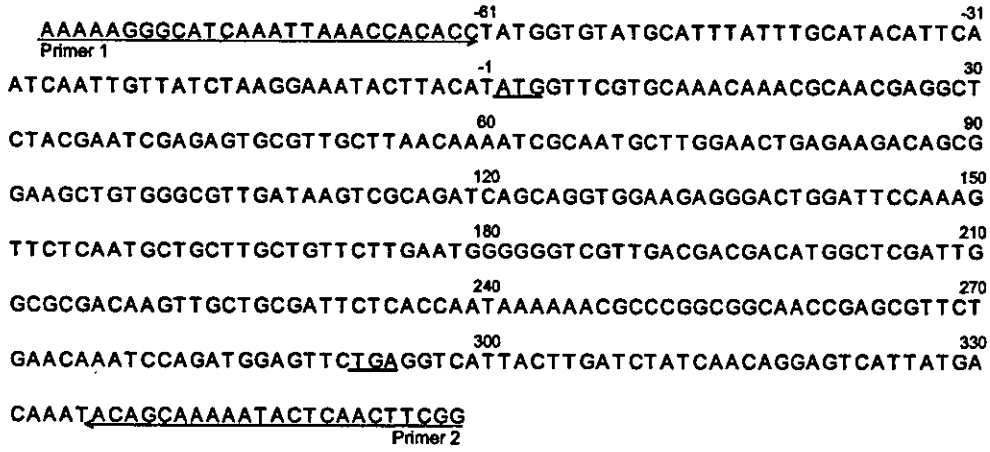

Fig. 3. Sequence map of the *cII* gene. The primers, used for PCR ampli. cation and sequencing, are shown by arrows. The PCR gives 446 bp products that involve the entire (294 bp) *cII* gene. Initiation and stop codons are underlined.

Table 1
Mutant frequencies induced by BfQ, BhQ and 1,7-Phe in . ve organs of Muta™Mouse for the expression time of 14 days

Tissue	Treatment	*lacZ* assay				*cII* assay			
		Individual animal data			Average ± S.D.	Individual animal data			Average ± S.D.
		No. of phages analyzed	No. of mutants	MF × 10^5	MF × 10^5	No. of phages analyzed	No. of mutants	MF × 10^5	MF × 10^5
Liver	Control (olive oil)	1120000	106	9.5	7.0 ± 1.6	449400	12	2.7	2.1 ± 0.6
		816000	59	7.2		938400	24	2.6	
		1198000	73	6.1		764400	11	1.4	
		791500	41	5.2		699000	11	1.6	
	BfQ	634500	32	5.0	9.6 ± 3.1	804600	12	1.5	3.8 ± 1.6
		590000	51	8.6		662400	35	5.3	
		158500	20	12.6		426300	23	5.4	
		221500	27	12.2		883200	28	3.2	
	BhQ	442000	29	6.6	5.9 ± 1.1	1188000	53	4.5	2.6 ± 1.1
		677000	39	5.8		1134600	21	1.9	
		257500	11	4.3		671700	17	2.5	
		645500	46	7.1		1011000	15	1.5	
	1,7-Phe	272000	41	15.1	15.9 ± 0.5**	813600	44	5.4	4.1 ± 0.8*
		183000	30	16.4		562800	19	3.4	
		263000	43	16.3		720000	25	3.5	
		184000	29	15.8		606000	25	4.1	
Spleen	Control (olive oil)	855500	116	13.6	7.3 ± 3.6	623100	12	1.9	2.4 ± 0.3
		533000	29	5.4		1502400	41	2.7	
		446500	25	5.6		546900	15	2.7	
		461000	22	4.8		569400	13	2.3	
	BfQ	210500	13	6.2	6.1 ± 0.6	2098200	25	1.2	3.5 ± 2.8
		244500	16	6.5		441000	13	2.9	
		403000	27	6.7		785400	65	8.3	
		256500	13	5.1		786600	13	1.7	
	BhQ	297000	12	4.0	6.5 ± 1.6	277800	10	3.6	2.9 ± 0.6
		354500	25	7.1		828300	22	2.7	
		396500	26	6.6		946200	31	3.3	
		544000	46	8.5		1608600	34	2.1	
	1,7-Phe	426500	34	8.0	7.0 ± 1.0	967200	20	2.1	2.4 ± 0.7
		502500	27	5.4		1023000	24	2.3	
		320000	24	7.5		1026900	16	1.6	
		462500	34	7.4		905400	32	3.5	
Lung	Control (olive oil)	1539500	127	8.2	6.0 ± 1.3	1027800	21	2.0	2.1 ± 0.4
		1111500	60	5.4		738000	21	2.8	
		678000	35	5.2		1142700	20	1.8	
		1473000	76	5.2		831600	15	1.8	
	BfQ	553000	39	7.1	6.0 ± 0.6	1107600	18	1.6	2.6 ± 0.6
		332000	18	5.4		903300	22	2.4	
		353000	21	5.9		1124700	36	3.2	
		266000	15	5.6		445200	14	3.1	
	BhQ	401500	51	12.7	10.8 ± 2.4*	1705500	37	2.2	3.5 ± 1.0
		481500	54	11.2		1071000	33	3.1	
		572500	72	12.6		2403000	99	4.1	
		372000	25	6.7		2083200	98	4.7	

Table 1 (*Continued*)

Tissue	Treatment	*lacZ* assay				*cII* assay			
		Individual animal data			Average ± S.D.	Individual animal data			Average ± S.D.
		No. of phages analyzed	No. of mutants	MF × 10^5	MF × 10^5	No. of phages analyzed	No. of mutants	MF × 10^5	MF × 10^5
	1,7-Phe	335500	29	8.6	10.3 ± 1.9*	1103400	26	2.4	2.9 ± 0.5
		351000	46	13.1		1012200	27	2.7	
		244500	27	11.0		909600	34	3.7	
		211000	18	8.5		892200	26	2.9	
Kidney	Control (olive oil)	219500	15	6.8	6.8 ± 1.4	551100	21	3.8	2.7 ± 1.0
		190000	17	8.9		426600	16	3.8	
		349500	17	4.9		588000	11	1.9	
		301000	20	6.6		771000	12	1.6	
	BfQ	682500	46	6.7	7.4 ± 1.1	1035000	25	2.4	3.9 ± 0.9
		550500	51	9.3		825000	36	4.4	
		474000	33	7.0		649800	30	4.6	
		484000	32	6.6		1599000	66	4.1	
	BhQ	920500	55	6.0	7.4 ± 1.2	1323600	26	2.0	2.2 ± 0.5
		622000	51	8.2		945000	27	2.9	
		113000	10	8.8		1408800	23	1.6	
		244500	16	6.5		1018200	23	2.3	
	1,7-Phe	486500	30	6.2	6.8 ± 0.5	814800	15	1.8	3.3 ± 1.6
		558000	38	6.8		660300	40	6.1	
		177000	12	6.8		520200	13	2.5	
		319500	24	7.5		1664700	48	2.9	
Bone marrow	Control (olive oil)	311000	32	10.3	7.1 ± 3.0	644100	14	2.2	1.3 ± 0.6
		465000	27	5.8		1041000	16	1.5	
		70500	2	2.8		111300	1	0.9	
		96500	9	9.3		154500	1	0.6	
	BfQ	325500	17	5.2	6.4 ± 0.9	1075200	16	1.5	2.6 ± 0.9
		256500	17	6.6		528000	12	2.3	
		326000	25	7.7		572100	22	3.8	
		708500	44	6.2		1144800	32	2.8	
	BhQ	257000	13	5.1	5.7 ± 0.5	1757100	20	1.1	1.7 ± 0.4
		617000	38	6.2		1349400	24	1.8	
		683000	41	6.0		1040400	22	2.1	
	1,7-Phe	502500	24	4.8	4.7 ± 0.5	963600	12	1.2	1.6 ± 0.6
		397500	19	4.8		962400	11	1.1	
		622000	33	5.3		1341000	21	1.6	
		332000	13	3.9		916900	24	2.6	

* Signi. cantly different from the control group, $P < 0.05$.
** Signi. cantly different from the control group, $P < 0.01$.

selection for *cII* mutants was performed according to the method of Jakubczak et al. [24] with slight modi-. cation as previously reported [14]. Brie. y, the phage solution was absorbed to *E. coli* G1225 (*h.* $^-$) at room temperature for 20–30 min. For titration, an appropriately diluted phage-*E. coli* solution was mixed with LB top agar (containing 10 mM $MgSO_4$), plated onto dishes containing bottom agar, and incubated for 24 h at 37 °C. The remaining phage-*E. coli* solution was mixed with LB top agar and plated onto dishes con-

Table 2
Mutant frequencies induced by BfQ and 1,7-Phe in . ve organs of Muta™Mouse for the expression time of 56 days

Tissue	Treatment	*lacZ* assay				*cII* assay			
		Individual animal data			Average ± S.D.	Individual animal data			Average ± S.D.
		No. of phages analyzed	No. of mutants	MF × 10^5	MF × 10^5	No. of phages analyzed	No. of mutants	MF × 10^5	MF × 10^5
Liver	Control (olive oil)	246500	21	8.5	7.9 ± 1.3	960700	18	1.9	1.7 ± 0.2
		168500	12	7.1		1161000	21	1.8	
		636500	39	6.1		3351900	65	1.9	
		155500	15	9.6		1978900	27	1.4	
	BfQ	259000	24	9.3	11.5 ± 2.8	543600	14	2.6	2.4 ± 0.2**
		367000	35	9.5		2746500	60	2.2	
		714000	116	16.2		3693000	97	2.6	
		180500	20	11.1		2490600	57	2.3	
	1,7-Phe	653000	63	9.6	14.8 ± 3.7*	1468200	64	4.4	4.8 ± 1.2**
		266500	35	13.1		1140000	36	3.2	
		497000	94	18.9		4469100	286	6.4	
		126000	22	17.5		306600	16	5.2	
Spleen	Control (olive oil)	608500	47	7.7	7.8 ± 0.4	1825800	53	2.9	2.9 ± 0.6
		347500	26	7.5		1304400	48	3.7	
		355500	30	8.4		1224600	36	2.9	
		389500	29	7.4		1106400	22	2.0	
	BfQ	440000	38	8.6	8.4 ± 0.3	2245800	32	1.4	3.3 ± 2.5
		242500	21	8.7		860400	14	1.6	
		354000	30	8.5		1090800	83	7.6	
		460500	36	7.8		946200	24	2.5	
	1,7-Phe	567000	81	14.3	10.0 ± 2.5	1022400	22	2.2	2.2 ± 0.04
		231500	18	7.8		976800	22	2.3	
		336000	29	8.6		1059000	23	2.2	
		253500	24	9.5		865800	19	2.2	
Lung	Control (olive oil)	390500	25	6.4	7.9 ± 1.9	657600	13	2.0	3.1 ± 0.9
		218500	21	9.6		1230600	30	2.4	
		558500	32	5.7		936000	35	3.7	
		474500	47	9.9		928800	38	4.1	
	BfQ	332500	26	7.8	7.2 ± 1.2	742200	19	2.6	3.7 ± 1.9
		554500	43	7.8		1035000	25	2.4	
		476000	39	8.2		839400	59	7.0	
		386000	20	5.2		651000	17	2.6	
	1,7-Phe	731500	56	7.7	7.7 ± 0.9	1365600	25	1.8	3.0 ± 0.9
		412000	32	7.8		728400	29	4.0	
		494500	44	8.9		966600	26	2.7	
		519000	33	6.4		946800	35	3.7	
Kidney	Control (olive oil)	442500	26	5.9	8.2 ± 2.4	1874400	64	3.4	2.5 ± 0.6
		217000	26	12.0		2313600	43	1.9	
		383000	25	6.5		1139400	25	2.2	
		596500	50	8.4		1437600	39	2.7	
	BfQ	552500	41	7.4	7.1 ± 1.0	1629600	60	3.7	2.9 ± 0.7
		479000	39	8.1		1360800	33	2.4	
		774500	56	7.2		1446000	50	3.5	
		698500	38	5.4		1277400	27	2.1	

Table 2 (*Continued*)

Tissue	Treatment	*lacZ* assay				*cII* assay			
		Individual animal data			Average ± S.D.	Individual animal data			Average ± S.D.
		No. of phages analyzed	No. of mutants	MF × 10^5	MF × 10^5	No. of phages analyzed	No. of mutants	MF × 10^5	MF × 10^5
	1,7-Phe	299500	19	6.3	7.3 ± 1.1	1201800	26	2.2	2.2 ± 0.3
		567500	50	8.8		1393200	35	2.5	
		877500	70	8.0		1409400	35	2.5	
		513500	32	6.2		1060200	19	1.8	
Bone marrow	Control (olive oil)	607500	43	7.1	7.9 ± 1.2	1334700	21	1.6	1.9 ± 0.4
		829000	57	6.9		1204800	25	2.1	
		924500	70	7.6		1441800	23	1.6	
		605500	60	9.9		1184400	30	2.5	
	BfQ	429000	26	6.1	6.9 ± 2.1	1703400	19	1.1	3.9 ± 4.1
		661500	69	10.4		1287600	15	1.2	
		893000	47	5.3		1256400	136	10.8	
		791500	45	5.7		1249200	29	2.3	
	1,7-Phe	605500	92	15.2	9.0 ± 3.8	1206600	13	1.1	1.5 ± 0.3
		447500	39	8.7		1700400	22	1.3	
		507000	30	5.9		876000	14	1.6	
		1188000	71	6.0		1444200	28	1.9	

* Signi. cantly different from the control group, $P < 0.05$.
** Signi. cantly different from the control group, $P < 0.01$.

taining bottom agar. The plates were incubated for 48 h at 25 °C for selection of *cII* mutants. The wild type phage, recovered from Muta^{TM}Mouse, has a *cI*$^-$ phenotype, which permits plaque formation with the *h.* $^-$ strain at 37 °C but not at 25 °C. The mutant frequency was calculated by the following formula:

$$\text{mutant frequency} = \left(\frac{\text{total number of plaques on selection plates}}{\text{total number of plaques on titer plates}}\right) \times \text{dilution factor.}$$

The signi. cance of differences in the mutant frequency between the treated and control groups was analyzed by using Student's *t*-test.

2.2.5. Sequencing of mutants

The entire lambda *cII* region was ampli. ed directly from mutant plaques by the use of Taq DNA polymerase (Takara Shuzo, Tokyo, Japan) with primers P1; 5′-AAAAAGGGCATCAAATTAAACC-3′, and P2; 5′-CCGAAGTTGAGTATTTTTGCTGT-3′ as previously reported [14] (Fig. 3). A 446 bp PCR product was puri. ed with a microspin column (Amersham Pharmacia, Tokyo, Japan) and then used for a sequencing reaction with the Ampli Taq cycle sequencing kit (PE Biosystems, Tokyo, Japan) using the primer P1. The reaction product was puri. ed by ethanol precipitation and analyzed with the ABI PRISM^{TM} 310 genetic analyzer (PE Biosystems).

3. Results

3.1. Mutant frequency of BfQ, BhQ, and 1,7-Phe

BfQ, BhQ, and 1,7-Phe (Fig. 1) were tested for in vivo mutagenicity using *lacZ* transgenic mice (Muta^{TM}Mice). The mutant frequencies observed in the DNA preparations extracted from the . ve organs are shown in Tables 1 and 2. Over 10 mutant plaques were analyzed in most organs. For the bone marrow in Table 1, the mutant frequency of one animal in the BhQ-treated group was missing and the number of mutants in two animals in the control group was insuf. cient because the isolated DNA was not enough

to be analyzed. The spontaneous mutant frequencies observed in the control group were similar for the . ve organs in both *lacZ* and *cII* assays regardless of the expression time (14 or 56 days), the rate ranging from 6.0 to 8.2 × 10^{-5} and from 1.3 to 3.1 × 10^{-5}, respectively. These results were similar to those of our previous studies [9,12–14].

Table 1 shows mutant frequencies with the test compounds in the . ve organs 14 days after the last injection. BfQ slightly, but not signi. cantly, increased the mutant frequency in the liver in both assays. On the other hand, BhQ signi. cantly increased the mutant frequency in the lung in the *lacZ* assay. 1,7-Phe signi. cantly increased the mutant frequency in the liver in both assays and in the lung in the *lacZ* assay.

Mutant frequencies observed in the DNA preparations extracted from the . ve organs 56 days after the last injection are shown in Table 2. BfQ signi. cantly increased the mutant frequency in the liver in the *cII* assay, whereas the mutant frequency in the *lacZ* assay was slightly, but not signi. cantly, increased. 1,7-Phe signi. cantly increased the mutant frequency in the liver in both assays like the results obtained 14 days

Table 3
Sequences of *cII* mutations in the liver of BfQ-treated Muta^{TM}Mouse for the expression time of 14 days

Mutant no.	Position	Mutation	Sequence	Amino acid change
A1	113	C to T	AAG TCG CAG	Ser to Leu
A2	99–100	GG to TT	GTG GGC GTT	Gly to Cys
A3	107	A to C	GTT GAT AAG	Asp to Ala
A4	57	C to G	CTT AAC AAA	Asn to Lys
A5	214	C to T	GCG CGA CAA	Arg to Stop
A6	181	G to T	TGG GGG GTC	Gly to Trp
A7	34	C to T	CTA CGA ATC	Arg to Stop
A8	103	G to A	GGC GTT GAT	Val to Ile
A9	196	G to T	GAC GAC ATG	Asp to Tyr
A10	129	G to C	AGG TGG AAG	Trp to Cys
A11	34	C to T	CTA CGA ATC	Arg to Stop
A12	25	G to A	AAC GAG GCT	Glu to Lys
A13	241–246	−A	AAA AAA CGC	Frameshift
A14	179–184	−G	TGG GGG GTC	Frameshift
A15	57	C to A	CTT AAC AAA	Asn to Lys
A16	35	G to T	CTA CGA ATC	Arg to Leu
A17	179–184	+G	TGG GGG GTC	Frameshift
A18	90–91	GG to TT	GCG GAA GCT	Glu to Stop
A19	94	G to T	GAA GCT GTG	Ala to Ser
A20	115	C to T	TCG CAG ATC	Gln to Stop
A21	193	G to A	GAC GAC GAC	Asp to Asn
A22	64	G to A	ATC GCA ATG	Ala to Thr
A23	103	G to A	GGC GTT GAT	Val to Ile
A24	104	T to C	GGC GTT GAT	Val to Ala
A25	89	C to T	ACA GCG GAA	Ala to Val
A26[a]	64	G to A	ATC GCA ATG	Ala to Thr
A27	175	G to T	CTT GAA TGG	Glu to Stop
A28	25	G to A	AAC GAG GCT	Glu to Lys
A29	34	C to T	CTA CGA ATC	Arg to Stop
A30	100	G to A	GTG GGC GTT	Gly to Ser
A31	62	T to C	AAA ATC GCA	Ile to Thr
A32[a]	25	G to A	AAC GAG GCT	Glu to Lys
A33	196	G to A	GAC GAC ATG	Asp to Asn
A34	179–184	−G	TGG GGG GTC	Frameshift
A35	115	C to A	TCG CAG ATC	Gln to Lys
A36	134	G to C	AAG AGG GAC	Arg to Thr

[a] Ascribable to the same mutation obtained in an identical mouse.

after the last injection. 1,7-Phe did not increase the mutant frequency in the lung for the expression time of 56 days.

3.2. Mutation spectra of BfQ, BhQ, and 1,7-Phe-induced mutations

A total of 36 BfQ-induced mutants in the liver for the expression time of 14 days, 37 BhQ-induced mutants in the lung for 14 days, and 43 1,7-Phe-induced mutants in the liver for 56 days were subjected to sequence analysis. The mutations are characterized in Tables 3–5, and summarized in Table 6. In Table 6, the same mutations in an identical mouse were treated as single events. The data of the spontaneous mutations are from our previous report [9].

1,7-Phe-induced mutations consisted mainly of base substitutions (36/39); G:C to A:T transitions (15/39) and G:C to C:G transversions (10/39) predominated. Compared with the spontaneous mutation spectrum, G:C to A:T transitions decreased and G:C to C:G transversions increased in the mutations by

Table 4
Sequences of *cII* mutations in the lung of BhQ-treated Muta™Mouse for the expression time of 14 days

Mutant no.	Position	Mutation	Sequence	Amino acid change
B1	196	G to A	GAC *G*AC ATG	Asp to Asn
B2	179–184	+G	T*GG GGG* GTC	Frameshift
B3	149	A to T	CCA *A*AG TTC	Lys to Met
B4	241–246	−A	*AAA AAA* CGC	Frameshift
B5	34	C to T	CTA *C*GA ATC	Arg to Stop
B6	113	C to T	AAG T*C*G CAG	Ser to Leu
B7	215	G to T	GCG C*G*A CAA	Arg to Leu
B8[a]	34	C to T	CTA *C*GA ATC	Arg to Stop
B9	166	G to C	CTT *G*CT GTT	Ala to Pro
B10	25	G to A	AAC *G*AG GCT	Glu to Lys
B11	34	C to T	CTA *C*GA ATC	Arg to Stop
B12	62	T to C	AAA A*T*C GCA	Ile to Thr
B13[a]	34	C to T	CTA *C*GA ATC	Arg to Stop
B14	233	T to C	ATT C*T*C ACC	Leu to Pro
B15	40	G to A	ATC *G*AG AGT	Glu to Lys
B16	212	C to T	TTG G*C*G CGA	Ala to Val
B17[a]	212	C to T	TTG G*C*G CGA	Ala to Val
B18	113	C to T	AAG T*C*G CAG	Ser to Leu
B19	46	G to C	AGT *G*CG TTG	Ala to Pro
B20	179–184	+G	T*GG GGG* GTC	Frameshift
B21	89	C to T	ACA G*C*G GAA	Ala to Val
B22	196	G to A	GAC *G*AC ATG	Asp to Asn
B23	190–198	−GAC	*GAC GAC GAC*	Frameshift
B24	34	C to T	CTA *C*GA ATC	Arg to Stop
B25	205	C to T	GCT *C*GA TTG	Arg to Stop
B26	179–184	−G	T*GG GGG* GTC	Frameshift
B27	122	G to T	ATC A*G*C AGG	Ser to Ile
B28	28	G to A	GAG *G*CT CTA	Ala to Thr
B29	52	C to G	TTG *C*TT AAC	Leu to Val
B30	197	A to G	GAC *G*AC ATG	Asp to Gly
B31	212	C to T	TTG G*C*G CGA	Ala to Val
B32	91	G to T	GCG *G*AA GCT	Glu to Stop
B33	205	C to T	GCT *C*GA TTG	Arg to Stop
B34	40	G to A	ATC *G*AG AGT	Glu to Lys
B35	34	C to T	CTA *C*GA ATC	Arg to Stop
B36[a]	40	G to A	ATC *G*AG AGT	Glu to Lys
B37	89	C to T	ACA G*C*G GAA	Ala to Val

[a] Ascribable to the same mutation obtained in an identical mouse.

Table 5
Sequences of *cII* mutations in the liver of 1,7-Phe-treated Muta™Mouse for the expression time of 56 days

Mutant no.	Position	Mutation	Sequence	Amino acid change
C1	113	C to T	AAG TCG CAG	Ser to Leu
C2	212	C to T	TTG GCG CGA	Ala to Val
C3	125	G to C	AGC AGG TGG	Arg to Thr
C4	196	G to A	GAC GAC ATG	Asp to Asn
C5	40	G to A	ATC GAG AGT	Glu to Lys
C6[a]	212	C to T	TTG GCG CGA	Ala to Val
C7	46	G to C	AGT GCG TTG	Ala to Pro
C8	94	G to C	GAA GCT GTG	Ala to Pro
C9	134	G to T	AAG AGG GAC	Arg to Met
C10	163	C to T	COG CTT GCT	Leu to Phe
C11	34	C to T	CTA CGA ATC	Arg to Stop
C12	179–240	−62 bp		Frameshift
C13	193	G to A	GAC GAC GAC	Asp to Asn
C14	65	C to T	ATC GCA ATG	Ala to Val
C15	164–165	−T	CTT GCT GTT	Frameshift
	166	G to A		
C16	1	A to G	cat ATG GTT	Met to Val
C17	224	C to A	GTT GCT GCG	Ala to Asp
C18	196	G to A	GAC GAC ATG	Asp to Asn
C19	150	G to T	CCA AAG TTC	Lys to Asn
C20	113	C to T	AAG TCG CAG	Ser to Leu
C21[a]	150	G to T	CCA AAG TTC	Lys to Asn
C22	129	G to A	AGG TGG AAG	Trp to Stop
C23	37	A to T	CGA ATC GAG	Ile to Phe
C24	140–141	GG to CT	GAC TGG ATT	Trp to Ser
C25	89	C to A	ACA GCG GAA	Ala to Glu
C26	34	C to T	CTA CGA ATC	Arg to Stop
C27	212	C to T	TTG GCG CGA	Ala to Val
C28	233	T to C	ATT CTC ACC	Leu to Pro
C29	28	G to C	GAG GCT CTA	Ala to Pro
C30	95	C to A	GAA GCT GTG	Ala to Asp
C31	89	C to G	ACA GCG GAA	Ala to Gly
C32	100	G to C	GTG GGC GTT	Gly to Arg
C33	25	G to T	AAC GAG GCT	Glu to Stop
C34	39	C to G	CGA ATC GAG	Ile to Met
C35	103	G to C	GGC GTT GAT	Val to Leu
C36	212	C to T	TTG GCG CGA	Ala to Val
C37	64	G to A	ATC GCA ATG	Ala to Thr
C38	193	G to T	GAC GAC GAC	Asp to Tyr
C39	95	C to A	GAA GCT GTG	Ala to Asp
C40	74	G to C	CTT GGA ACT	Gly to Ala
C41	120	C to G	CAG ATC AGC	Ile to Met
C42[a]	39	C to G	CGA ATC GAG	Ile to Met
C43[a]	64	G to A	ATC GCA ATG	Ala to Thr

[a] Ascribable to the same mutation obtained in an identical mouse.

1,7-Phe. On the other hand, BfQ and BhQ-induced *cII* mutant spectra showed no characteristics compared with that of the control and consisted mainly of G:C to A:T transitions (15/34 and 18/33, respectively).

4. Discussion

In this study, we attempted to investigate the in vivo mutagenicity of three tricyclic aza-arenes, BfQ, BhQ, and 1,7-Phe. They were injected daily for 4 days

Table 6
Summary of *cII* mutation spectra in Muta™Mouse

Mutation class	Control[a] (%)	BfQ[b] (%)	BhQ[c] (%)	1,7-Phe[b] (%)
Total	32 (100)	34 (100)	33 (100)	39 (100)
Base substitution	28 (88)	28 (82)	28 (85)	36 (92)
Transitions				
GC to AT	18 (56)	15 (44)	18 (55)	15 (38)
AT to GC	1 (3)	2 (6)	3 (9)	2 (5)
Transversions				
AT to TA	3 (9)	0 (0)	1 (3)	1 (3)
AT to CG	0 (0)	1 (3)	0 (0)	1 (3)
GC to TA	5 (16)	7 (20)	3 (9)	7 (18)
GC to CG	1 (3)	3 (9)	3 (9)	10 (26)
−1 frameshifts	1 (3)	3 (9)	2 (6)	0 (0)
+1 frameshifts	2 (6)	1 (3)	2 (6)	0 (0)
Deletion	0 (0)	0 (0)	1 (3)	1 (3)
Insertion	0 (0)	0 (0)	0 (0)	0 (0)
Complex	1 (3)	2 (6)	0 (0)	2 (5)

The same mutations from an identical mouse were counted as single events.
[a] The data of the spontaneous mutations are from our previous report [9].
[b] Mutant plaques from the liver.
[c] Mutant plaques from the lung.

into Muta™Mice at the total doses of 400, 400, and 200 mg/kg intraperitoneally, respectively, based on their tolerance doses determined in preliminary tests. Although these aza-analogs of phenanthrene were weak mutagens in Muta™Mouse, different effects on the target organ speci. city and mutant spectrum were observed depending on the N-substituted position.

BfQ increased the mutant frequency in the liver for the expression times of both 14 and 56 days. On the other hand, BhQ increased mutagenicity in the lung, but not in the liver. BfQ has a nitrogen atom in the bay-region and BhQ in the non-bay-region. Therefore, the difference in the nitrogen position in the benzoquinoline molecule might alter the target organ. Quinoline has previously shown a potent in vivo mutagenicity in Muta™Mice [12–14]. These results suggest that in vivo mutagenicity is decreased by the benzene-ring fusion on the quinoline moiety. 1,7-Phe signi. cantly increased mutagenicity in the liver for the expression times of both 14 and 56 days and in the lung for the expression time of 14 days. It may be suggested that 1,7-Phe induced mutation both in the liver and lung because 1,7-Phe has a nitrogen atom in both the bay- and non-bay-regions. Our previous data indicated that metabolic activation of these phenanthrene aza-analogs might take place in the pyridine moiety [18] (Fig. 2). LaVoie and co-workers reported that BfQ might be converted to the ultimate form not only by the bay-region mechanism but also by another mechanism [17], supporting our opinion.

With regard to the suitable expression time in the evaluation of in vivo mutagenicity, different tendencies were observed between the mutagenesis of 1,7-Phe in the liver and that in the lung. 1,7-Phe showed similar mutagenicities in the liver after the expression time of both 14 and 56 days. However, in the lung, 1,7-Phe increased the mutant frequency in the lung after the expression time of 14 days, but not after 56 days. Sun and Heddle reported that mutation by ethylnitrosourea in the liver was more . rmly established after about 40 days post-treatment than after 20 days [25]. It seems that an appropriate expression time may be necessary to evaluate the in vivo mutagenicity of chemicals in each organ.

1,7-Phe also depressed the G:C to A:T transition and increased the G:C to C:G transversion like quinoline [14], a hepatomutagen possessing the partial structure of 1,7-Phe, compared with the spontaneous mutation spectrum. Therefore it may be suggested that the increase of G:C to C:G transversions might be a common feature of the quinoline-type metabolic activation in aza-arenes.

Although a major question to be answered is how the position of the nitrogen atom is responsible for the differences in mutagenicity between these tricyclic aza-arenes, the present data suggest that the position of the nitrogen atom in the polycyclic aromatic ring might in. uence in vivo mutagenicity with respect to the target organ speci. city and mutational pattern.

Acknowledgements

We thank Dr. T. Nohmi for his kind gifts of *E. coli* NM759 and BHB2688, and Dr. K. Masumura for his technical guidance in making packaging extracts. This research is supported in part by the grant from the Ministry of Environment, Japan.

References

[1] I. Schmeltz, D. Hoffmann, Nitrogen-containing compounds in tobacco and tobacco smoke, Chem. Rev. 77 (1977) 295–311.
[2] M. Dong, D.C. Locke, D. Hoffmann, Characterization of aza-arenes in basic organic portion of suspended particulate matter, Environ. Sci. Technol. 11 (1977) 612–618.
[3] C.R. Engel, E. Sawicki, A superior thin-layer chromatographic procedure for the separation of aza arenes and its application to air pollution, J. Chromatogr. 31 (1967) 109–119.
[4] D. Brocco, A. Cimmino, M. Possanzini, Determination of azaheterocyclic compounds in atmospheric dust by a combination of thin-layer and gas chromatography, J. Chromatogr. 84 (1973) 371–377.
[5] A. Lacassagne, N.P. Buu-Hoi, F. Zajdela, P. Mabille, Carcinogenic activity of some isosteric nitrogenous pentacyclic hydrocarbon carcinogens, Compt. Rend. 258 (1964) 3387–3389.
[6] Y. Kitahara, H. Okuda, K. Shudo, T. Okamoto, M. Nagao, Y. Seino, T. Sugimura, Synthesis and mutagenicity of 10-azabenzo[*a*]pyrene-4,5-oxide and other pentacyclic aza-arene oxides, Chem. Pharm. Bull. (Tokyo) 26 (1978) 1950–1953.
[7] H. Okuda, Y. Kitahara, K. Shudo, T. Okamoto, Identi. cation of an ultimate mutagen of 10-azabenzo[*a*]pyrene: microsomal oxidation of 10-azabenzo[*a*]pyrene to 10-azabenzo[*a*]pyrene-4,5-oxide, Chem. Pharm. Bull. (Tokyo) 27 (1979) 2547–2549.
[8] C.H. Ho, B.R. Clark, M.R. Guerin, B.D. Barkenbus, T.K. Rao, J.L. Epler, Analytical and biological analysis of test materials from the synthetic fuel technologies, Mutat. Res. 85 (1981) 335–345.
[9] K. Yamada, T. Suzuki, A. Kohara, M. Hayashi, A. Hakura, T. Mizutani, K.I. Saeki, Effect of 10-aza-substitution on benzo[*a*]pyrene mutagenicity in both in vivo and in vitro, Mutat. Res. 521 (2002) 187–200.
[10] K. Hirao, Y. Shinohara, H. Tsuda, S. Fukushima, M. Takahashi, Carcinogenic activity of quinoline on rat liver, Cancer Res. 36 (1976) 329–335.
[11] Y. Shinohara, T. Ogiso, M. Hananouchi, K. Nakanishi, T. Yoshimura, N. Ito, Effect of various factors on the induction of liver tumors in animals by quinoline, Jpn. J. Cancer Res. 68 (1977) 785–796.
[12] T. Suzuki, Y. Miyata, K.I. Saeki, Y. Kawazoe, M. Hayashi, T. Sofuni, In vivo mutagenesis by the hepatocarcinogen quinoline in the *lacZ* transgenic mouse: evidence for its in vivo genotoxicity, Mutat. Res. 412 (1998) 161–166.
[13] Y. Miyata, K.I. Saeki, Y. Kawazoe, M. Hayashi, T. Sofuni, T. Suzuki, Antimutagenic structure modi. cation of quinoline assessed by an in vivo mutagenesis assay using *lacZ*-transgenic mice, Mutat. Res. 414 (1998) 165–169.
[14] T. Suzuki, X. Wang, Y. Miyata, K.I. Saeki, A. Kohara, Y. Kawazoe, M. Hayashi, T. Sofuni, Hepatocarcinogen quinoline induces G:C to C:G transversions in the *cII* gene in the liver of lambda/*lacZ* transgenic mice (MutaMouse), Mutat. Res. 456 (2000) 73–81.
[15] R.S. Baker, A.M. Bonin, I. Stupans, G.M. Holder, Comparison of rat and guinea pig as sources of the S9 fraction in the *Salmonella*/mammalian microsome mutagenicity test, Mutat. Res. 71 (1980) 43–52.
[16] G.M. Seixas, B.M. Andon, P.G. Hollingshead, W.G. Thilly, The aza-arenes as mutagens for *Salmonella typhimurium*, Mutat. Res. 102 (1982) 201–212.
[17] S. Kumar, H.C. Sikka, S.K. Dubey, A. Czech, N. Geddie, C.X. Wang, E.J. LaVoie, Mutagenicity and tumorigenicity of dihydrodiols, diol epoxides, and other derivatives of benzo(*f*)quinoline and benzo(*h*)quinoline, Cancer Res. 49 (1989) 20–24.
[18] K.I. Saeki, H. Kawai, Y. Kawazoe, A. Hakura, Dual stimulatory and inhibitory effects of . uorine-substitution on mutagenicity: an extension of the enamine epoxide theory for activation of the quinoline nucleus, Biol. Pharm. Bull. 20 (1997) 646–650.
[19] M. Dong, I. Schmeltz, E. LaVoie, D. Hoffmann, Aza-arenes in the respiratory environment: analysis and assays for mutagenicity, in: P.W. Jones, R.I. Freudenthal (Eds.), Carcinogenesis: A Comprehensive Survey, vol. 3, Raven, New York, 1978, pp. 97–108.
[20] E.A. Adams, E.J. LaVoie, D. Hoffmann, Mutagenicity and metabolism of azaphenanthrenes, in: M.C. Cooke, A.J. Dennis (Eds.), Polynuclear Aromatic Hydrocarbons, Formation, Metabolism, and Measurement, Battelle Press, Columbus, OH, 1983, pp. 73–87.
[21] W.C. Summers, P.M. Glazer, D. Malkevich, Lambda phage shuttle vectors for analysis of mutations in mammalian cells in culture and in transgenic mice, Mutat. Res. 220 (1989) 263–268.
[22] E.J. Gunther, N.E. Murray, P.M. Glazer, High ef. ciency, restriction-de. cient in vitro packaging extracts for bacteriophage lambda DNA using a new *E. coli* lysogen, Nucleic Acids Res. 21 (1993) 3903–3904.

[23] J.A. Gossen, A.C. Molijn, G.R. Douglas, J. Vijg, Application of galactose-sensitive *E. coli* strains as selective hosts for *LacZ*-plasmids, Nucleic Acids Res. 20 (1992) 3254.

[24] J.L. Jakubczak, G. Merlino, J.E. French, W.J. Muller, B. Paul, S. Adhya, S. Garges, Analysis of genetic instability during mammary tumor progression using a novel selection-based assay for in vivo mutations in a bacteriophage lambda transgene target, Proc. Natl. Acad. Sci. U.S.A. 93 (1996) 9073–9078.

[25] B. Sun, J.A. Heddle, The relationship between mutant frequency and time in vivo: simple predictions for any tissue, cell type, or mutagen, Mutat. Res. 425 (1999) 179–183.

Environmental and Molecular Mutagenesis 43:186–195 (2004)

DNA Adducts and Mutagenic Specificity of the Ubiquitous Environmental Pollutant 3-Nitrobenzanthrone in Muta Mouse

Volker M. Arlt,[1]* Li Zhan,[2] Heinz H. Schmeiser,[3] Masamitsu Honma,[2] Makoto Hayashi,[2] David H. Phillips,[1] and Takayoshi Suzuki[2]

[1] *Section of Molecular Carcinogenesis, Institute of Cancer Research, Surrey, United Kingdom*

[2] *Division of Genetics and Mutagenesis, National Institute of Health Sciences, Tokyo, Japan*

[3] *Division of Molecular Toxicology, German Cancer Research Center, Heidelberg, Germany*

3-nitrobenzanthrone (3-NBA) is an extremely potent mutagen in the Salmonella reversion assay and a suspected human carcinogen identified in diesel exhaust and in ambient airborne particulate matter. To evaluate the in vivo mutagenicity of 3-NBA, we analyzed the mutant frequency (MF) in the *cII* gene of various organs (lung, liver, kidney, bladder, colon, spleen, and testis) in lambda/*lacZ* transgenic mice (Muta Mouse) after intraperitoneal treatment with 3-NBA (25 mg/kg body weight injected once a week for 4 weeks). Increases in MF were found in colon, liver, and bladder, with 7.0-, 4.8-, and 4.1-fold increases above the control value, respectively, whereas no increase in MF was found in lung, kidney, spleen, and testis. Simultaneously, induction of micronuclei in peripheral blood reticulocytes was observed. The sequence alterations in the *cII* gene recovered from 41 liver mutants from 3-NBA-treated mice were compared with 32 spontaneous mutants from untreated mice. Base substitution mutations predominated for both the 3-NBA-treated (80%) and the untreated (81%) groups. However, the proportion of G:C→T:A transversions in the mutants from 3-NBA-treated mice was higher (49% vs. 6%) and the proportion of G:C→A:T transitions was lower than those from untreated mice (10% vs. 66%). The increase in MF in the liver was associated with strong DNA binding by 3-NBA, whereas in lung, in which there was no increase in MF, a low level of DNA binding was observed (268.0–282.7 vs. 8.8–15.9 adducts per 10^8 nucleotides). DNA adduct patterns with multiple adduct spots, qualitatively similar to those formed in vitro after activation of 3-NBA with nitroreductases and in vivo in rats, were observed in all tissues examined. Using high-pressure liquid cochromatographic analysis, we confirmed that all major 3-NBA-DNA adducts produced in vivo in mice are derived from reductive metabolites bound to purine bases (70–80% with deoxyguanosine and 20–30% with deoxyadenosine in liver). These results suggest that G:C→T:A transversions induced by 3-NBA are caused by misreplication of adducted guanine residues through incorporation of adenine opposite the adduct (A-rule). Environ. Mol. Mutagen. 43: 186–195, 2004.

Key words: 3-nitrobenzanthrone; Muta Mouse; mutation spectra; *cII*; DNA adducts; ^{32}P-postlabeling; diesel exhaust; air pollution; nitropolycyclic aromatic hydrocarbon

INTRODUCTION

Air pollution from diesel exhaust is an increasing concern as an environmental risk factor for carcinogenesis [World Health Organization, 2003]. Diesel exhaust is known to induce tumors in experimental animals and epidemiological studies have shown that occupational exposure to diesel exhaust is associated with an increased risk of lung cancer in humans [International Agenecy for Research on Cancer, 1989; Boffeta et al., 2001]. Nitropolycyclic aromatic hydrocarbons (nitro-PAHs) are widely distributed environmental pollutants found in airborne particulate matter, especially that emitted from diesel and gasoline engines [Tokiwa and Ohnishi, 1986; Yaffe et al., 2001]. Many members of this class of compounds are potent mutagens and carcinogens and their detection in the lungs of nonsmokers with lung

Grant sponsor: Cancer Research U.K.; Grant sponsor: Baden-Württemberg; Grant number: BWPLUS, BWB2003.

*Correspondence to: Volker M. Arlt, Section of Molecular Carcinogenesis, Institute of Cancer Research, Brookes Lawley Building, Cotswold Road, Sutton, Surrey SM2 5NG, United Kingdom. E-mail: volker.arlt@icr.ac.uk

Received 30 October 2003; provisionally accepted 22 November 2003; and in final form 24 January 2004

DOI 10.1002/em.20014

Published online in Wiley InterScience (www.interscience.wiley.com).